Probing Li Ion Dynamics in Amorphous $xLi_2SO_4 \cdot (1\text{-}x)LiPO_3$ by Quasielastic Neutron Scattering

Tom Heitmann[a,*], Gavin Hester[b], Saibal Mitra[b], Thomas Calloway[b], Madhu Tyagi[c], Andrew Miskowiec[d], Souleymane Diallo[d], Naresh Osti[d], Eugene Mamontov[d]

[a] *the Missouri Research Reactor, University of Missouri, Columbia, MO, USA*
[b] *Department of Physics, Astronomy, and Materials Science, Missouri State University, Springfield, MO, USA*
[c] *NIST Center for Neutron Research, National Institute of Standards and Technology, Gaithersburg, MD, USA*
[d] *Oak Ridge National Laboratory, Oak Ridge, TN, USA*

Abstract

The diffusion dynamics of a series of lithium sulfate substituted phosphate glass materials $xLi_2SO_4 \cdot (1\text{-}x)LiPO_3$ has been probed by quasielastic neutron scattering. Amorphous Li ion conductors are attractive as electrolyte materials for all-solid state batteries because they are highly isotropic and chemically stable. Local disorder is expected to reduce barriers to ion migration– leading to improved ionic conductivity relative to their crystalline counterpart– while minimizing unwanted electron transport. We report Li self-diffusion in these materials on a length scale comparable to the interatomic spacings, obtaining values $D \simeq 55 \pm 4$ x 10^{-8} cm^2/s at 450 K. Elastic neutron scattering measurements show an alteration of the phosphate chain backbone of the glass material.

Keywords: Li diffusion, quasielastic neutron scattering, solid electrolyte

1. Introduction

Portable electronic devices coupled with a growing electric vehicle market are currently driving an escalating need for improved energy storage devices[1]. For the past several decades Li ion batteries have provided rechargeable energy storage for laptops, cell phones, hand-held power tools, and the like. At the same time, electric cars are becoming more available, yet their battery packs continue to be a significant weight and financial burden[2]. Increasing prevalence of renewable energy sources further underscore the need for a next generation energy storage that is scalable, rapid charging, high energy density, and stable. The stability and scalability are related in the sense that one limitation to scaling Li ion batteries is the risk of runaway chemical reactions of the flammable, liquid organic based

*Corresponding author
Email address: HeitmannT@missouri.edu (Tom Heitmann)

electrolyte that is prone to forming dendritic shorts. From this perspective it is clear that device gains can be made by improved component materials, notably with the electrolyte.

One approach is to replace the liquid electrolyte with a solid one. The primary advantage is that a solid state electrolyte is impervious to the kind of dendrite formation that have led to various well publicized incidents of battery combustion[3]. A wide array of candidate materials have been considered, including solid polymer[4], polycrystalline[5], and amorphous electrolytes[6][7][8]. Each have their advantages, however, we focus on one particular subset of amorphous electrolyte materials and, in particular, set our sights on the fundamental diffusion properties of these materials as a test base for the broader scope of amorphous ionic conductors.

Amorphous solid electrolytes have been put forward as an attractive option based on their isotropic conduction properties, favorable chemical stability, and the idea that introducing defects creates ionic conduction pathways of lower diffusive jump potential barriers[9]. *Ab initio* molecular dynamics simulations point to a hopping mechanism in which the Li ion is passed from one neighboring O atom to the next and reveals a reduced activation potential compared to its crystalline counterpart[10]. Our aim is to probe this local jumping via quasielastic neutron scattering (QENS) in amorphous phosphate glass materials with Li-salt additions, providing some tuning for the level of disorder present in the material. Our chosen matrix is amorphous $LiPO_3$ with Li_2SO_4 as the salt addition: xLi_2SO_4·(1-x)$LiPO_3$. These materials have been shown to increase in conductivity with added Li_2SO_4 up to $x = 0.6$, reaching conductivities as high as 10^{-6} S/cm. Above this value Li_2SO_4 crystallites begin to form and the conductivity is degraded[11]. This precipitate crystal formation indicates the presence of phase segregation as described by the cluster-tissue model[12]. Then, a central question in the performance of these materials is, what is the relative importance of the medium range order and the local jump diffusion dynamics? Bulk diffusion measurements, for example, yields a value of 6.0 x 10^{-13} cm^2/s for a lithium phosphate glass of a different stoichiometry Li_3PO_4[13]. In this work, we utilize quasielastic neutron scattering in order to assess the Li ionic diffusion on a local scale.

Quasielastic neutron scattering is a powerful technique for studying diffusion dynamics. It is a technique that has primarily been applied to hydrogen diffusion because of the unusu-ally high incoherent neutron scattering cross section for H, $\sigma_{inc} = 80.3$ barn. This property tends to produce strong QENS signal. For ^{7}Li the incoherent cross section is non-zero, but two orders of magnitude smaller than hydrogen ($\sigma_{inc} = 0.8$ barn), making it difficult but possible. Furthermore, the high thermal neutron absorption cross section for ^{6}Li ($\sigma_{abs} = 940$ barn) makes isotopic enrichment with ^{7}Li an advantage whenever possible. The primary advantage of QENS is that the technique allows access to the diffusion dynamics on time and length scales that match with the local diffusion jump steps. QENS has been applied to Li ion diffusion, but with comparatively fewer examples. Kamazawa et al.[14] have applied the QENS technique to measure the self diffusion of Li in lithium ion battery cathode mate-

rials $^7LiMn_2O_4$ and $^7Li_{1.1}Mn_{1.9}O_4$. The diffusion constant for each was found to be several orders of magnitude greater than what has been reported by NMR, pointing to an importance of length and time scales in the diffusion process. Anode materials have also been studied by QENS. Sacci et al.[15] have found the diffusion constant in Li_xSi to be 3 x 10^{-6} cm^2/s, also much greater than previously reported for the material. Crystalline garnet-type oxides[16][17][18] and $Li_7P_3S_{11}$[19] have also been measured by QENS. Some of us have also reported on QENS measurements of other members of the same $xLi_2SO_4{\cdot}(1\text{-}x)LiPO_3$ series, albeit in a more narrow energy range[20]. In there, we also observed Lorentzian broadening, however, the Q-dependence suggested site hopping dynamics, which we do not see in the present work, perhaps because of some variation in the glass microstructure or because of the varied time and length scales probed on the different instruments. These QENS studies have been enabled by developments in neutron backscattering instrumentation as well as more powerful neutron sources, notably the Spallation Neutron Source at Oak Ridge National Laboratory.

In this paper, we present the results of neutron backscattering measurements of representative members of the Li electrolyte glass series: $xLi_2SO_4{\cdot}(1\text{-}x)LiPO_3$; x = 0, 0.05, 0.3, and 0.4.

2. Experimental

Phosphate glass samples with composition $xLi_2SO_4{\cdot}(1\text{-}x)LiPO_3$ ranging from $x = 0$ to 0.6 were prepared by conventional melt-quenching a mixture of high purity powders of lithium sulfate (Li_2SO_4), ammonium dihydrogen phosphate ($NH_4H_2PO_4$) and lithium carbonate (Li_2CO_3). Three compositions (x = 0.05, 0.3, and 0.4) were prepared using 99% isotopically pure $^7Li_2SO_4$ and $^7Li_2CO_3$. Appropriate amounts of the powders were weighed and mixed in a porcelain crucible that was then placed in a preheated furnace at 450 °C. After an hour, the temperature of the furnace was then raised to 900 °C. Once the furnace reached the desired temperature, the crucible was removed and the melt was quenched between two copper plates. The resulting glass was crushed using a pestle and mortar.

Quasielastic neutron scattering measurements were performed on approximately 5 g of the ^7Li enriched $xLi_2SO_4{\cdot}(1\text{-}x)LiPO_3$ for x = 0.05, 0.3, and 0.4 on the backscattering spectrometer (BASIS)[21] at the Spallation Neutron Source. A natural abundance sample of x = 0 was measured also on BASIS and the disk chopper spectrometer (DCS)[22] of the NIST Center for Neutron Research. In each case, the sample was arranged in an annular geometry by forming a sachet of powdered sample in food-grade aluminum foil. The powder in foil sachet was then lined on the inside diameter of a 2.9 cm aluminum can for the BASIS measurements and a 1.7 cm one for DCS. The samples were kept in an inert atmosphere prior to measurement owing to concerns over water vapor absorption. The elastic scattering was checked for each sample to verify a low presence of H. The backscattering spectrum at 50 K was measured and in each case used as a measure of instrumental resolution. Empty sample cell measurements– including the aluminum foil– were used for background subtraction from each signal spectrum at the same temperature. The samples were then measured at elevated temperatures in the closed-cycle refrigerator furnace at 520 K for x = 0 and

450 K for the others. Temperatures were chosen to enhance self-diffusion while avoiding the glass transition temperature such that the material structure was unchanged during the measurement process. We used Si (111) analyzers on BASIS in the asymmetric mode to achieve a total energy range of -120 μeV to 520 μeV and a resolution of 3.5 μeV. The DCS was operated with a wavelength of $\lambda = 9$ Å in the medium resolution mode resulting in a resolution of ~ 12 μeV.

Each of these samples– as well as compositions of $x = 0.2$ and 0.6– were subsequently measured on the triple-axis spectrometer (TRIAX) at the University of Missouri Research Reactor (MURR) in the elastic configuration. These measurements were performed at room temperature while the sample was contained in a 1.27 cm diameter cylindrical aluminum sample cell sealed with a helium environment. A pyrolytic graphite (PG) (002) monochromator was used with $E_i = E_f = 14.7$ meV, which allows for a Q-range up to 4.5 Å^{-1}. Empty sample cell measurements were again subtracted from the signal data to obtain the elastic structure factor S(Q).

3. Results and Discussion

The energy resolved elastic window of the backscattering spectrum provides a measure of atomic motions that are slower than the instrumental resolution ($\sim$1 ns on BASIS). This energy scale translates to a mean square displacement for atoms in the system, as is plotted in Fig. 1, as a function of temperature. A linear dependence in the low temperature range results from the harmonic vibrations of atoms about their equilibrium position as described by the Debye-Waller factor, $W = \mathrm{e}^{-Q^2<u^2>/6}$ where $< u^2 >$ is the mean square displacement. Deviations from this linear behavior indicate anharmonic motions, which we identify with translational diffusion of the Li ions present in the system. Such a deviation is observed for both $x = 0.3$ and 0.4 in the vicinity of room temperature. Therefore, the diffusive dynamics in the QENS are expected to be observable above this temperature. Note that because our lowest temperature data point was taken at 50 K, there is an arbitrary offset to the overall mean square displacement.

The QENS was measured at 450 K for each of these two compositions. The resulting QENS spectrum is shown in Fig. 2. The spectrum fitting was performed using the NIST Data Analysis and Visuilization Environment software (DAVE)[23]. Diffusive motions of the Li ions result in a broadening of the incoherent central peak. The contribution to the background resulting from the sample holder was subtracted from the signal. A flat background was included in the fitting in order to account for any fast component contribution from the sample itself. The resolution was captured by measuring a low temperature (50 K) backscattering spectrum for each sample. The resolution was then convoluted with a delta function to account for the difference in scattering intensity for the sample. The remaining signal was then fit to a Lorentzian peak, expected for diffusion dynamics, resulting from the Fourier transform of a Gaussian distribution of randomly diffusing ions. We do not attempt any analysis of whether this line shape is correct for this system as the statistical limitations of QENS on Li do not support such a line shape analysis. The results of fitting the $x =$

0.4 sample at $T = 450$ K and $Q = 0.9$ Å^{-1} is shown in Fig. 2. A weak QENS broadening resulting from Li ion diffusion was detected for both $x = 0.3$ and 0.4 compositions at 450 K.

The Q-dependence of the Lorentzian full width at half maximum Γ carries information of the local diffusion process. A linear dependence with Q^2 indicates isotropic translational diffusion, where the slope is a direct measure of the diffusion constant, $\Gamma = 2DQ^2$. We plot Γ vs. Q^2 in Fig. 3 for $x = 0.3$ and 0.4. We note that diffusion for these two compositions is the same within our statistical precision, with a diffusion constant $D \simeq 55 \pm 4$ x 10^{-8} cm^2/s.

Two samples on the low Li_2SO_4 content end of the composition range ($x = 0$ and 0.05) were also measured via backscattering spectroscopy and disk chopper time-of-flight spectroscopy. For these compositions, no QENS signal above the instrumental background was observed, indicating that either the diffusion dynamics in these materials is below the resolution limit of both the BASIS and DCS instruments or, more likely, that an insufficient fraction of the Li ions are mobile so that no signal is achieved. Either scenario points to the enhancement in ionic conductivity with increasing Li_2SO_4 content as observed in conductivity measurements[6].

We have further studied the short range structure of these and two other compositions within the Li_2SO_4 solubility range, $x = 0.2$ and 0.6, via elastic neutron scattering on TRIAX at MURR. The signal is energy resolved using a flat PG (002) analyzer set to the same energy as the incident neutrons, such that only the neutrons that are elastic within the resolution window of 0.65 meV are detected. The Q-dependent structure factors $S(Q)$ are shown in Fig. 4. A double peak feature is observed for the low x compositions with peaks near $Q = 1.2$ and 1.7 Å^{-1}. Suzuya et al.[24] reported such a double peak feature for a range of alkali phosphate glasses, including a lithium metaphosphate, which is the same as our $x = 0$ composition.

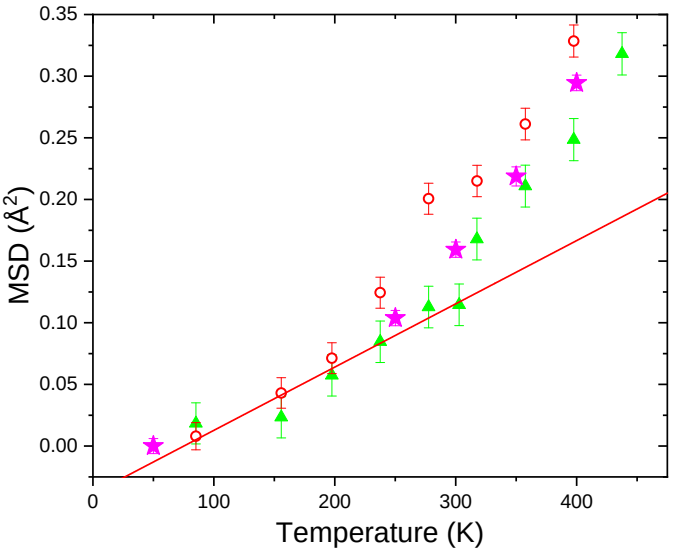

Figure 1: (Color online) The elastic component of the backscattering signal is monitored as a function of temperature to obtain the mean square displacement. Open red circles: x = 0.3; Green triangles and magenta stars (from higher statistics spectra): x = 0.4.

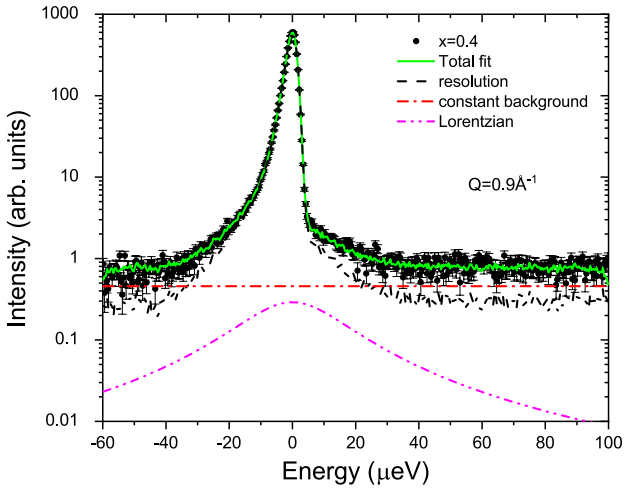

Figure 2: (Color online) QENS signal and Lorentizian fitting for x = 0.4 at 450 K on BASIS. An empty sample cell measurement at 450 K was subtracted off to account for their contribution to the background. An additional flat background term was included in the fitting in order to account for any fast processes in the sample that fall outside of the instrumental dynamic range. Then, low temperature data (50 K) was taken as the instrumental resolution and convoluted with a delta function. The remaining signal was fit with a Lorentzian to obtain the broadening resulting from Li diffusion.

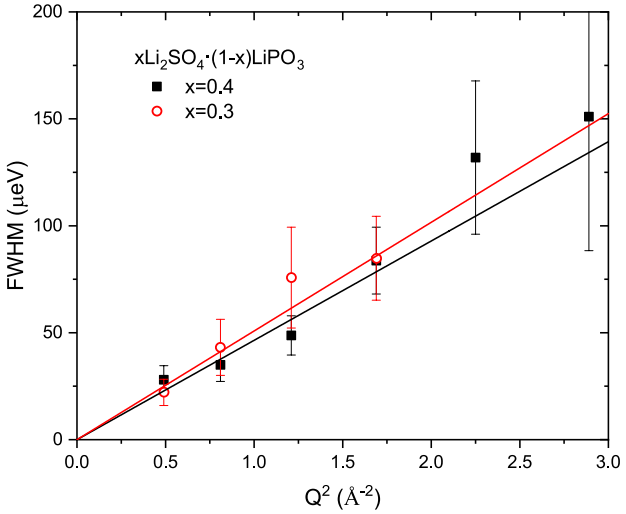

Figure 3: (Color online) The quasielastic broadening is plotted vs. Q^2 to demonstrate the quadratic behavior, indicating isotropic translational diffusion in the length- and time-scales that are proved in the measurement.

The peak originates from a periodicity in the disordered structure on a length scale of 5 Å, which is frequently termed intermediate range order in glass materials. The double peak structure indicates the presence of two distinct orders in the intermediate range structure. Interestingly, the lower-Q peak at 1.2 $Å^{-1}$ diminishes as more Li_2SO_4 is added. At the same time, the peak at 1.7 $Å^{-1}$ becomes stronger and more sharp. This can be understood as

a perforating of the phosphate chain network, leaving increasingly truncated chains until order along the chain structure is lost. Such an interpretation is born out by recent *ab initio* molecular dynamics simulations[10]. Suzuya et al.[24] applied a model of random packing structural units as a useful simplification of the related vitreous P_2O_5, whereby P_4O_{10} molecules were taken to populate a psuedo-b.c.c. lattice. One pertinent observation that they made was that the strength of the so called pre-peak is strongly dependent upon whether the P_4O_{10} molecules are oreintationally ordered or not, where a high degree of orientational order results in a strong peak. By applying this model to our elastic data on TRIAX, we are able to index the three main peak features to a pseudo-b.c.c. lattice of a $\simeq$ 7.4 Å, which is very similar to what Suzuyu et al. used for the vitreous P_2O_5 case. The peaks are indexed as follows: q = 1.2 $Å^{-1}$ corresponds to (110); q = 1.7 $Å^{-1}$, (200); and, q = 2.7 $Å^{-1}$, (310). The (220) is also an allowed reflection in this range and is expected at q $\simeq$ 2.4 $Å^{-1}$. We propose that as Li_2SO_4 is introduced, the perforating of the P_2O_5 backbone that runs along the pseudo-b.c.c lattice diagonal results in an additional degree of rotational freedom for the P_4O_{10} molecules such that orientational order is lost and with it a reduction in the elastic intensity for the (110) and (220) reflections, resulting in an overall increased sharpness of the surrounding (200) and (310) peaks that are relatively unaffected by the orientational properties of the P_4O_{10} molecules.

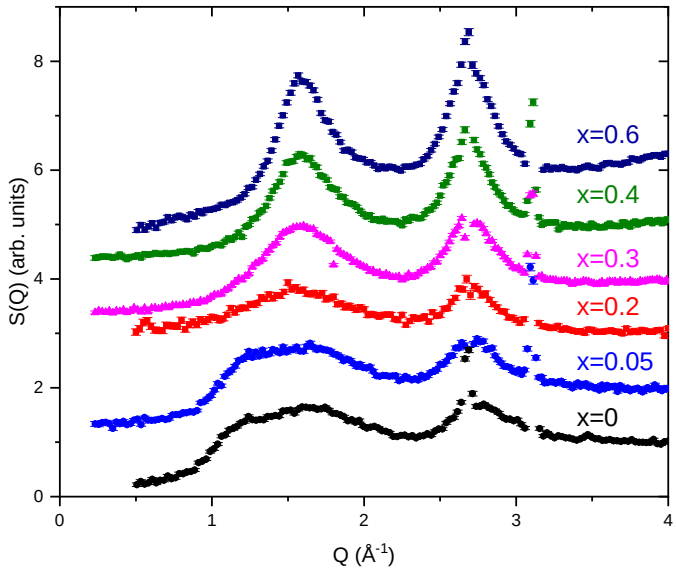

Figure 4: (Color online) Elastic structure factor as measured on TRIAX. A dramatic evolution of the low Q double peak feature illustrates an important modulation of the intermediate range order in the amorphous $LiPO_3$ matrix.

In any case, it is clear that dramatic changes are happening to the structure on these length scales. It is natural to expect these changes to manifest in the diffusion dynamics and raises the question as to where gains can be made in material performance with respect to engineering faster hopping dynamics or whether the length scales of intermediate range order or cluster-tissue type structure are more important. QENS is nevertheless a crucial

tool for the understanding of the fundamental hopping process in the quest to disambiguate the contributions from these different length scales.

4. Conclusions

The diffusion coefficient ($D \simeq 55 \pm 4$ x 10^{-8} cm^2/s) for two members of the amorphous Li electrolyte materials xLi_2SO_4·(1-x)$LiPO_3$ (x = 0.3 and 0.4) have been determined via quasielastic neutron scattering on the BASIS backscattering spectrometer at Oak Ridge National Laboratory. Compositions of $x = 0$ and 0.05 were also measured on BASIS as well as DCS at the NIST Center for Neutron Research, however, no discernable signal above background was observed. We attribute this fact to a comparatively small number of mobile ions at the measurement temperature, consistent with the improved ionic conductivity of the higher Li_2SO_4 content compositions. An alteration of the intermediate range structure was observed by elastic neutron scattering measurements on TRIAX at MURR. These measurements suggest a diminished level of ordering along the phosphate chains, likely resulting in a more isoptropic diffusion.

Acknowledgements

We acknowledge the support of the National Institute of Standards and Technology, U.S. Department of Commerce, in providing the neutron research facilities used in this work. A portion of this research used resources at the Spallation Neutron Source, a DOE Office of Science User Facility operated by the Oak Ridge National Laboratory.

References

[1] B. Scrosati, J. Garche, Lithium batteries: Status, prospects and future, Journal of Power Sources 195 (9) (2010) 2419 – 2430. doi:https://doi.org/10.1016/j.jpowsour.2009.11.048.
[2] R. Van Noorden, A better battery, Nature 507 (7490) (2014) 26.
[3] K. Liu, Y. Liu, D. Lin, A. Pei, Y. Cui, Materials for lithium-ion battery safety, Science Advances 4 (6). doi:10.1126/sciadv.aas9820.
[4] L. Long, S. Wang, M. Xiao, Y. Meng, Polymer electrolytes for lithium polymer batteries, J. Mater. Chem. A 4 (2016) 10038–10069. doi:10.1039/C6TA02621D.
[5] C. Cao, Z.-B. Li, X.-L. Wang, X.-B. Zhao, W.-Q. Han, Recent advances in inorganic solid electrolytes for lithium batteries, Frontiers in Energy Research 2 (2014) 25. doi:10.3389/fenrg.2014.00025.
[6] M. Rathore, A. Dalvi, Crystallization in Li_2SO_4–Li_2O–P_2O_5 glassy ionic system: An assessment through electrical transport, Journal of Non-Crystalline Solids 402 (2014) 79–83.
[7] M. Ganguli, M. H. Bhat, K. Rao, Lithium ion transport in Li_2SO_4–Li_2O–P_2O_5 glasses, Solid State Ionics 122 (1-4) (1999) 23–33.
[8] J. Bates, N. Dudney, G. Gruzalski, R. Zuhr, A. Choudhury, C. Luck, J. Robertson, Fabrication and characterization of amorphous lithium electrolyte thin films and rechargeable thin-film batteries, Journal of Power Sources 43 (1 -3 pt 1) (1993) 103–110. doi:10.1016/0378-7753(93)80106-Y.
[9] J. C. Dyre, P. Maass, B. Roling, D. L. Sidebottom, Fundamental questions relating to ion conduction in disordered solids, Reports on Progress in Physics 72 (4) (2009) 046501.
[10] M. S. Islam, P. Simanjuntak, S. Mitra, R. Sakidja, DFT study on the Li mobility in Li-ion-based solid-state electrolytes, MRS Advances 2 (54) (2017) 3277–3282.

[11] M. Rathore, A. Dalvi, Electrical transport in Li_2SO_4–Li_2O–P_2O_5 ionic glasses and glass–ceramic composites: A comparative study, Solid State Ionics 239 (2013) 50–55.
[12] M. Aniya, J. Kawamura, Medium range structure and activation energy of ion transport in glasses, Solid State Ionics 154 (2002) 343–348.
[13] N. Kuwata, X. Lu, T. Miyazaki, Y. Iwai, T. Tanabe, J. Kawamura, Lithium diffusion coefficient in amorphous lithium phosphate thin films measured by secondary ion mass spectroscopy with isotope exchange methods, Solid State Ionics 294 (2016) 59 – 66. doi:https://doi.org/10.1016/j.ssi.2016.06.015.
[14] K. Kamazawa, H. Nozaki, M. Harada, K. Mukai, Y. Ikedo, K. Iida, T. J. Sato, Y. Qiu, M. Tyagi, J. Sugiyama, Interrelationship between Li^+ diffusion, charge, and magnetism in $^7LiMn_2O_4$ and $^7Li_{1.1}Mn_{1.9}O_4$ spinels: Elastic, inelastic, and quasielastic neutron scattering, Physical Review B 83 (9) (2011) 094401.
[15] R. L. Sacci, M. L. Lehmann, S. O. Diallo, Y. Q. Cheng, L. L. Daemen, J. F. Browning, M. Doucet, N. J. Dudney, G. M. Veith, Lithium transport in an amorphous Li_xSi anode investigated by quasi-elastic neutron scattering, The Journal of Physical Chemistry C 121 (21) (2017) 11083–11088.
[16] H. Nozaki, M. Harada, S. Ohta, N. H. Jalarvo, E. Mamontov, I. Watanabe, Y. Miyake, Y. Ikedo, J. Sugiyama, Diffusive behavior of Li ions in garnet $Li_{5+x}La_3Zr_xNb_{2-x}O_{12}$ (x= 0–2), Journal of the Physical Society of Japan 82 (Suppl. A) (2013) SA004.
[17] H. Nozaki, M. Harada, S. Ohta, I. Watanabe, Y. Miyake, Y. Ikedo, N. H. Jalarvo, E. Mamontov, J. Sugiyama, Li diffusive behavior of garnet-type oxides studied by muon-spin relaxation and QENS, Solid State Ionics 262 (2014) 585–588.
[18] M. J. Klenk, S. E. Boeberitz, J. Dai, N. H. Jalarvo, V. K. Peterson, W. Lai, Lithium self-diffusion in a model lithium garnet oxide $Li_5La_3Ta_2O_{12}$: A combined quasi-elastic neutron scattering and molecular dynamics study, Solid State Ionics 312 (2017) 1 – 7. doi:https://doi.org/10.1016/j.ssi.2017.09.022.
[19] K. Mori, K. Enjuji, S. Murata, K. Shibata, Y. Kawakita, M. Yonemura, Y. Onodera, T. Fukunaga, Direct observation of fast lithium-ion diffusion in a superionic conductor: $Li_7P_3S_{11}$ metastable crystal, Physical Review Applied 4 (5) (2015) 054008.
[20] G. Hester, T. Heitmann, M. Tyagi, M. Rathore, A. Dalvi, S. Mitra, Neutron scattering studies of lithium-ion diffusion in ternary phosphate glasses, MRS Advances 1 (45) (2016) 3057–3062.
[21] E. Mamontov, K. W. Herwig, A time-of-flight backscattering spectrometer at the spallation neutron source, BASIS, Review of Scientific Instruments 82 (8) (2011) 085109.
[22] J. Copley, J. Cook, The disk chopper spectrometer at NIST: a new instrument for quasielastic neutron scattering studies, Chemical Physics 292 (2) (2003) 477 – 485, quasielastic Neutron Scattering of Structural Dynamics in Condensed Matter. doi:https://doi.org/10.1016/S0301-0104(03)00124-1.
[23] R. T. Azuah, L. R. Kneller, Y. Qiu, P. L. Tregenna-Piggott, C. M. Brown, J. R. Copley, R. M. Dimeo, DAVE: a comprehensive software suite for the reduction, visualization, and analysis of low energy neutron spectroscopic data, Journal of Research of the National Institute of Standards and Technology 114 (6) (2009) 341.
[24] K. Suzuya, D. L. Price, C.-K. Loong, S. W. Martin, Structure of vitreous P_2O_5 and alkali phosphate glasses, Journal of Non-Crystalline Solids 232 (1998) 650–657.

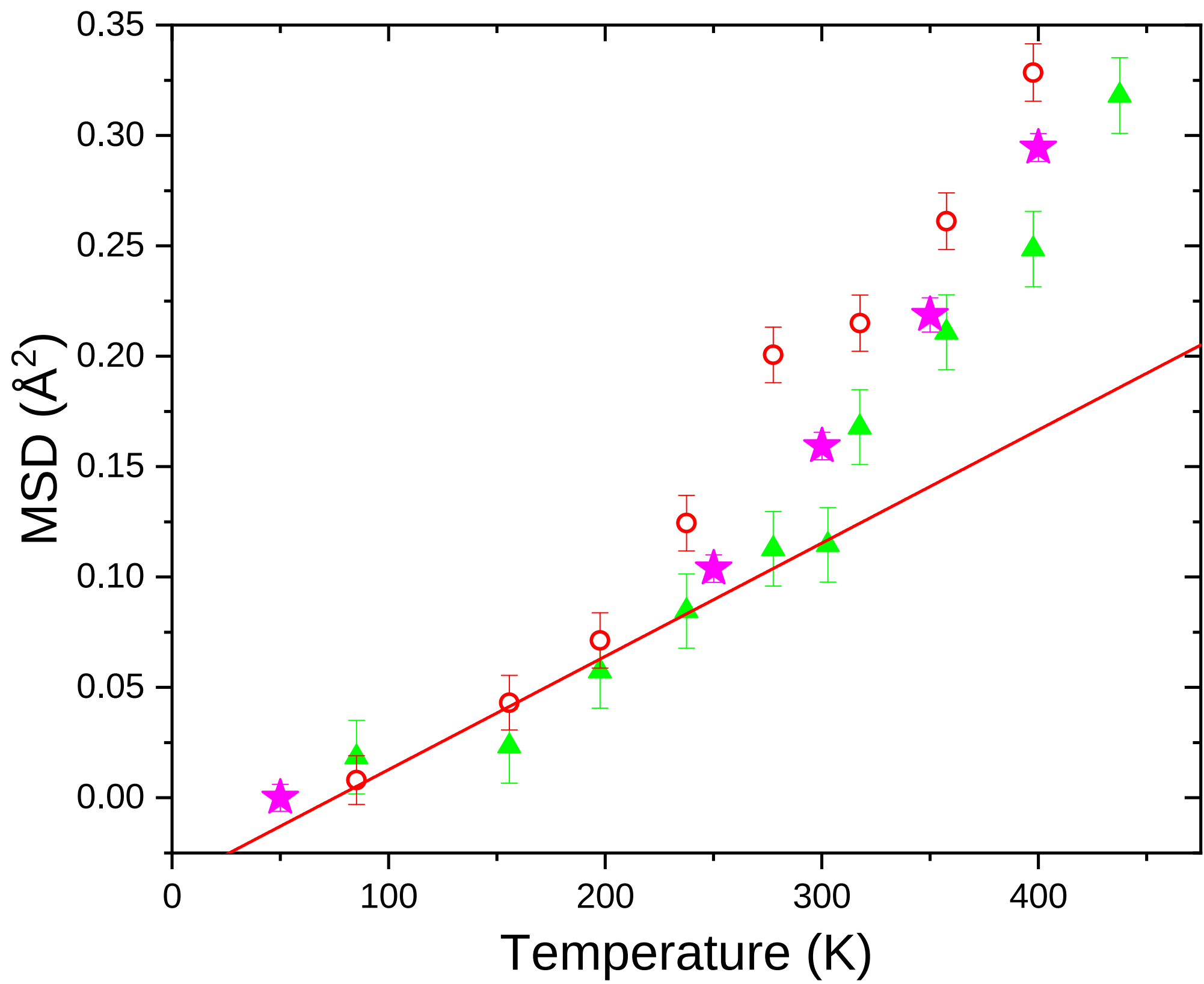
0.35
0.30
0.25
0.20
0.15
0.10
0.05
0.00
MSD (Å^2)
0
100
200
300
400
Temperature (K)

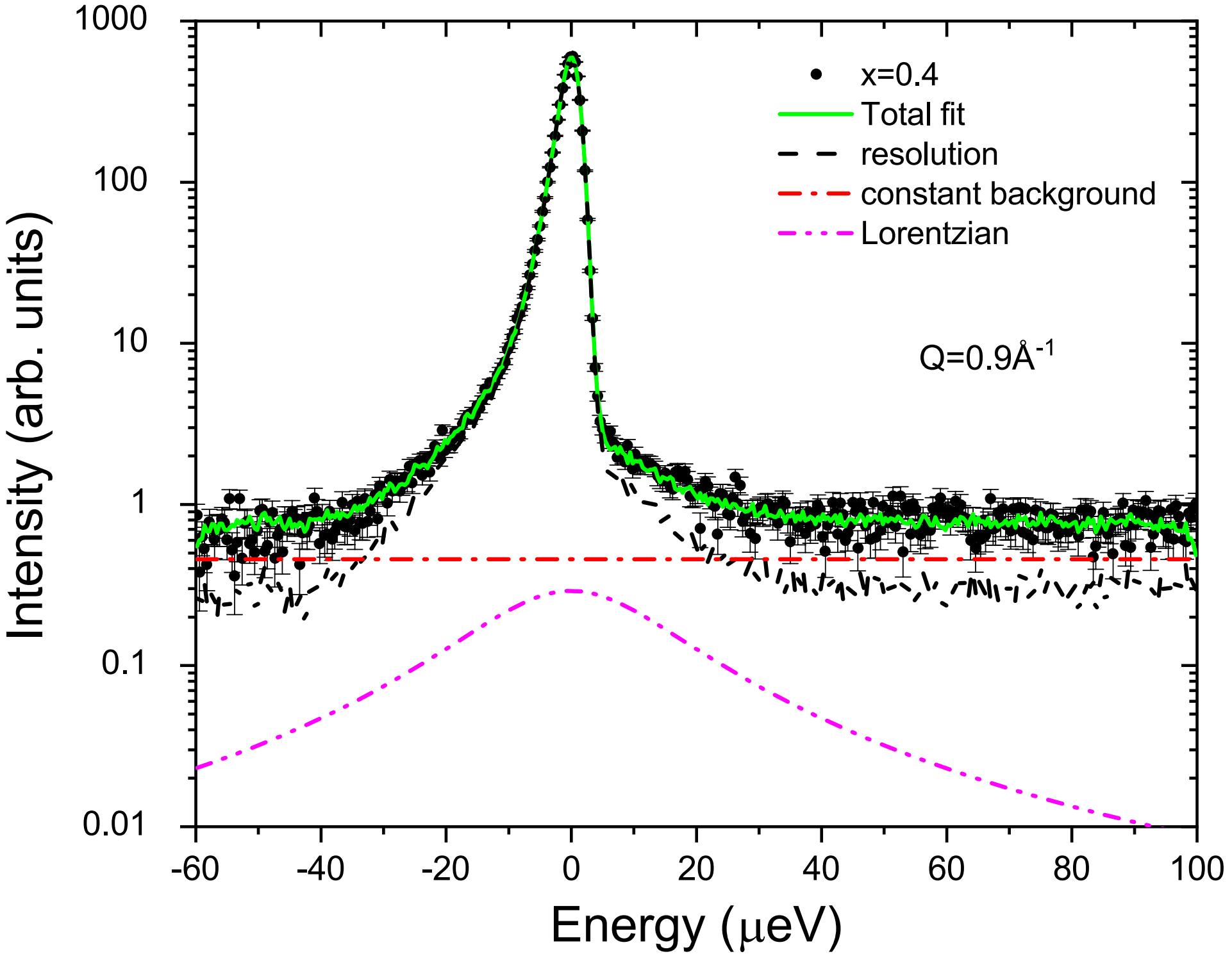
1000
100
10
1
0.1
0.01
Intensity (arb. units)
-60
-40
-20
0
20
40
60
80
100
Energy (μeV)
x=0.4
Total fit
resolution
constant background
Lorentzian
Q=0.9Å-1

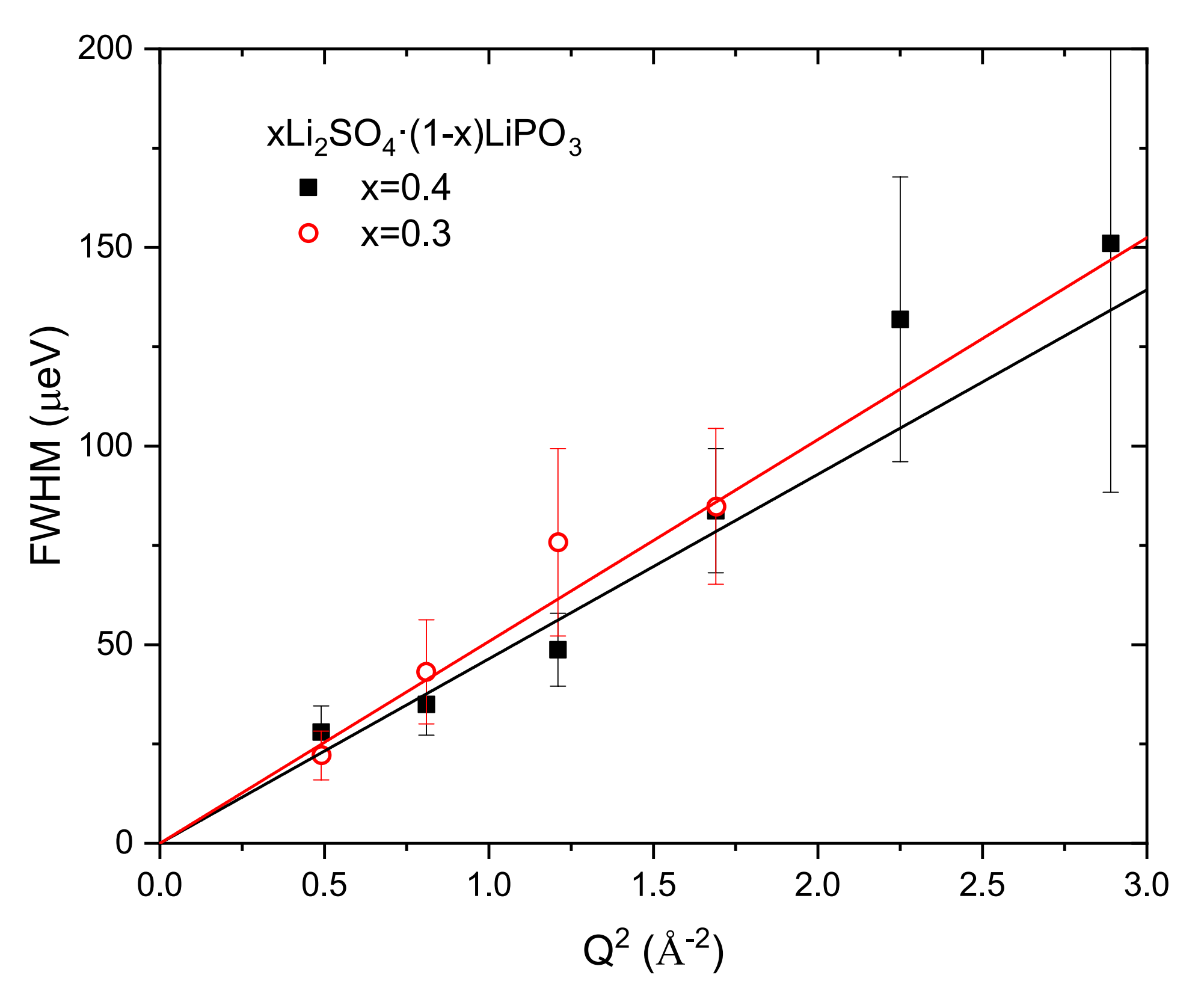
xLi2SO4·(1-x)LiPO3
x=0.4
x=0.3
FWHM (μeV)
Q2 (Å-2)
0
50
100
150
200
0.0
0.5
1.0
1.5
2.0
2.5
3.0

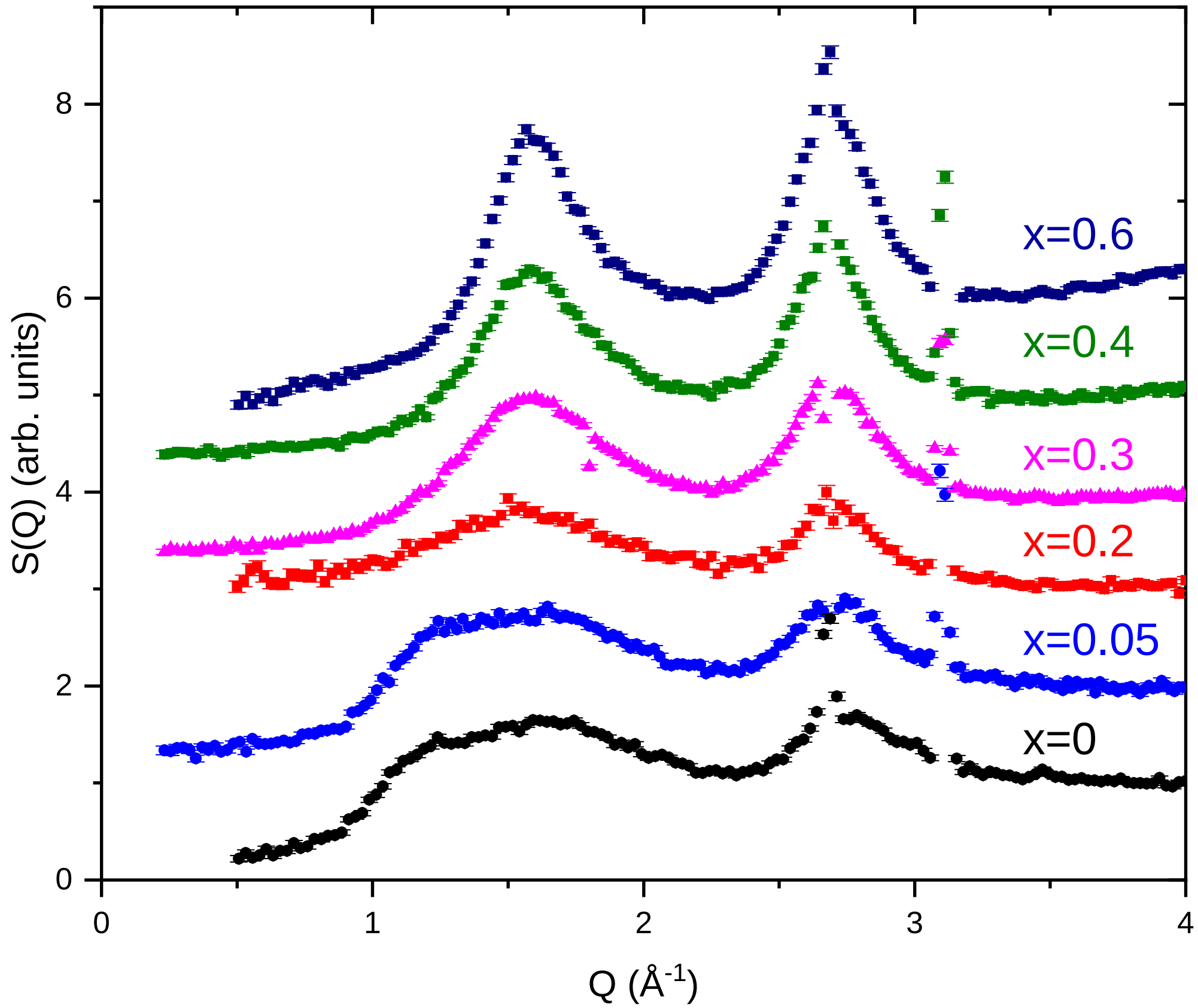
S(Q) (arb. units)
Q (Å^{-1})
0
2
4
6
8
0
1
2
3
4
x=0.6
x=0.4
x=0.3
x=0.2
x=0.05
x=0